DINAME 2017 - Proceedings of the XVII International Symposium on Dynamic Problems of Mechanics
A. T. Fleury, D. A. Rade, P. R. G. Kurka (Editors), ABCM, São Sebastião, SP, Brazil, March 5-10, 2017

Implementation and analysis of a navigation system for autonomous underwater vehicles

Rodrigo E. Y. Diana[1], **Ettore A. de Barros**[2]

[1] Mechatronics Engineering Department, Polytechnic School, University of São Paulo, 05508-030, São Paulo, SP, Brazil. (Tel: +55-11-98386-2020; e-mail: ro.diana@usp.br)

[2] Mechatronics Engineering Department, Polytechnic School, University of Sao Paulo, 05508-030, São Paulo, SP, Brazil. (Tel: +55-11-3091-6017; e-mail: eabarros@usp.br)

Abstract: This document proposes a navigation system for position estimation of AUVs using the principle of dead reckoning and followed by an analytical expression to predict its accumulated positioning error based on maneuvers duration and the embedded navigation sensors specifications. The position estimation can be expressed both in a local and geodesic frames, which permits correlating the collected oceanographic data and trajectory to maps. The algorithm is tested using real navigation data and the trajectory is plotted using real maps for visualization. Practical issues are then discussed, such as magnetic declination correction and improvement of velocity measurement and prediction. The algorithm position estimation is compared to the embedded GPS signal, defining its error. The error is then compared to the predicted one by the analytical expression, verifying its applicability to foresee error accumulation during the absence of GPS signal on underwater missions.

Keywords: AUV, navigation system, dead reckoning, error estimation, signal filtering

NOMENCLATURE

Latin symbols

$\mathbf{R}_b^n$: rotation matrix from frame b to n
$\boldsymbol{p}$: vehicle's position vector
$\boldsymbol{v}$: vehicle's velocity vector
$\boldsymbol{a}$: vehicle's acceleration vector
$\boldsymbol{f}$: vehicle's specific force vector
L: latitude
d: vehicle's depth

Greek symbols

$\boldsymbol{\Theta}$: vehicle's attitude (Euler angles) vector
$\boldsymbol{\Omega}$: Earth's rotation vector
ϕ: vehicle's roll
θ: vehicle's pitch
ψ: vehicle's yaw
λ: longitude

Subscripts and notations

e: subscript for geodesic frame
n: subscript for local navigation frame
b: subscript for body frame
$\hat{\bullet}$: notation for estimation of $\bullet$
$\delta\bullet$: notation for error of $\bullet$
$c\bullet$: notation for $cos(\bullet)$
$s\bullet$: notation for $sin(\bullet)$

INTRODUCTION

AUVs (Autonomous Underwater Vehicles) are cheaper and smaller than real submarines. They are also easier to transport and does not require a pilot, so they have been used to perform various missions on the late 40 years, like for oceanographic studies, military and oil & gas industries (Paull, 2014). Today, there are a few dozen of commercial AUVs. The Laboratory of Unmanned Vehicles of the Polytechnic School of the University of São Paulo, Brazil, started in 2008 the AUV Pirajuba project. Thenceforth, it has carried out researches on hydrodynamics (Barros, 2008 and Caetano, 2014), control architecture (Freire, 2013) and Kalman filtering for state estimation (Zanoni, 2012, Vivanco, 2014). The vehicle is now operational and equipped with sensors, which are necessary for its autonomous navigation. Missions to collect oceanographic data, related to the detection and identification of plankton in the northern coastline of São Paulo state, have been successfully conducted. The navigation of the vehicle is performed by its trajectory control system, which is composed by four subsystems with different tasks (figure 1).

- Navigation system: linear and angular position estimation.
- Trajectory planner: defines continuously the next way-point to follow.
- Guidance system: produces the velocity and attitude references.
- Autopilot: generates the commands for the rudders, elevators and propellant.

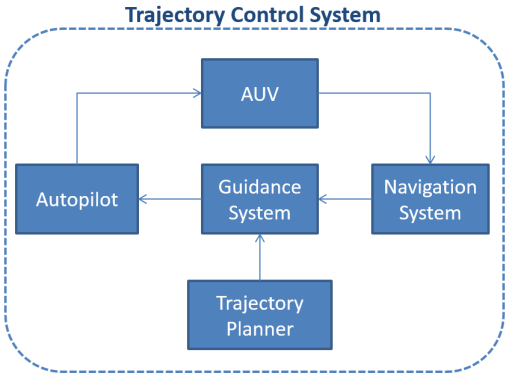

Figure 1 – Trajectory Control System.

The vehicle's control and autonomy depends on a precise position estimation by the navigation system. Also, the collected oceanographic data usually must be correlated with the geodesic coordinate of the vehicle, another important task that depends on it, knowing that there is no GPS signal underwater.

This paper presents an implementation of a navigation system for AUVs with position estimation expressed in a local navigation frame and global geodesic frame. The algorithm is applied on the Pirajuba AUV. To evaluate the precision of the position estimation algorithm, an analytical expression of the accumulated positioning error is developed. It considers the maneuvers duration and the precision of the navigation sensors, provided by the manufactures, to obtain a theoretical error. It is then compared to the real error, which is the difference between the final position estimation by the algorithm and by the GPS, once the vehicle have emerged. The maneuvers are plotted using the Google Earth tool (Google, 2016) for visualization.

1 DEVELOPMENT OF A NAVIGATION SYSTEM FOR AUVS

Most of the AUVs, including the Pirajuba AUV, have the following navigation sensors embedded:

- GPS: measures the geodesic position (lack of signal underwater).
- Depth gauge: measures the depth.
- DVL (Doppler Velocity Logger): measures the linear velocity.
- IMU (Inertial Measurement Unit): measures the angular velocity and linear acceleration.
- AHRS (Attitude and Heading Reference System): estimates the attitude (angular position).

Using the information provided by those sensors, it is possible to implement an algorithm that estimates continuously the linear position of the vehicle.

1.1 Navigation equations

In this paper, the navigation system uses the dead reckoning principle, which estimates the current position recursively based on the previous estimation. For that, a time integration of the velocity is processed, as show on figure 2.

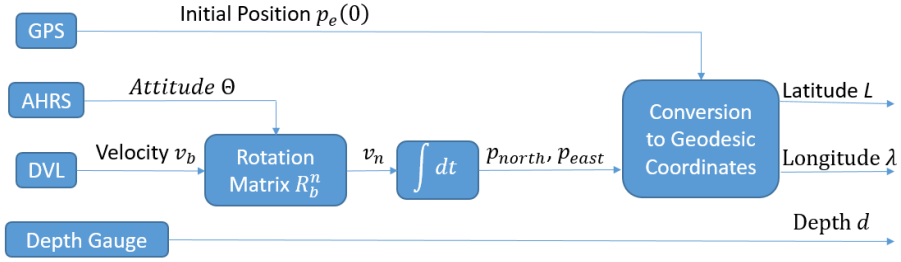

Figure 2 – Navigation algorithm schema using the dead reckoning principle.

In order to obtain the vehicle's geodesic coordinates $(L, \lambda, d)^T$, the local position $(p_{east}, p_{north}, p_{down})^T$, expressed on the local navigation frame n, must be calculated first. The origin of n may be placed anywhere on the surface of the Earth. In this paper, it is coincident with the start point of the maneuver, on the surface of the sea. Its X axis (north) points towards the geographic north, the Y axis (east) towards east and the Z axis (down) to the center of the Earth, defining a LTP (Local Tangent Plane) reference system. Since the DVL velocity sensor axes are attached to the vehicle's frame b,

a base rotation operation, represented by the $\mathbf{R_b^n}$ matrix, is needed, converting the measured velocity $\boldsymbol{v_b}$ in b frame to n. Matrix $\mathbf{R_b^n}$ uses the Euler angles $(\phi, \theta, \psi)^T$, provided by the AHRS sensor, as input.

$$\boldsymbol{p_n}(t) = \begin{pmatrix} p_{north}(t) \\ p_{east}(t) \\ p_{down}(t) \end{pmatrix} = \int_0^t \boldsymbol{v_n}(\tau).d\tau + \boldsymbol{p_n}(0) \tag{1}$$

where

$$\boldsymbol{v_n}(t) = \begin{pmatrix} v_{north}(t) \\ v_{east}(t) \\ v_{down}(t) \end{pmatrix} = \mathbf{R_b^n}(\boldsymbol{\Theta}(t)).\boldsymbol{v_b}(t) \text{ and } \mathbf{R_b^n}(\boldsymbol{\Theta}) = \begin{pmatrix} c\psi.c\theta & -s\psi.c\phi + c\psi.s\theta.s\phi & s\psi.s\phi + c\psi.c\phi.s\theta \\ s\psi.c\theta & c\psi.c\phi + s\phi.s\theta.s\psi & -c\psi.s\phi + s\theta.s\psi.c\phi \\ -s\theta & c\theta.s\phi & c\theta.c\phi \end{pmatrix},$$

$$c\bullet = cos(\bullet),\ s\bullet = sen(\bullet),\ \boldsymbol{v_b}(t) = \begin{pmatrix} u(t) \\ v(t) \\ w(t) \end{pmatrix},\ \boldsymbol{\Theta}(t) = \begin{pmatrix} \phi(t) \\ \theta(t) \\ \psi(t) \end{pmatrix}$$

Thanks to the fact that the vehicle still has GPS signal on the origin of n, since it is on the surface of the sea, the conversion of P_n to geodesic coordinate frame e is possible. Yet, some hypothesis must be considered:

- The distances covered by the AUV are much smaller than Earth's radius, which permits considering it locally flat.
- The Z axis of n is perpendicular to the tangent plane defined by the X and Y axis.
- Earth has an ellipsoid format as stated by the WGS84 system.

The WGS (World Geodetic System) 84 is the reference coordinate system used by the GPS. It approximates Earth's shape by an ellipsoid with origin on the Earths's center of mass, major radius R_0 of 6 378 137.0 m and with eccentricity factor e of 0.0818191908425. On most of the surface of the ellipsoid, the normal to the tangent plane does not intercepts the origin. Hence, there are two different definitions for the latitude: geodesic and geocentric (figure 3).

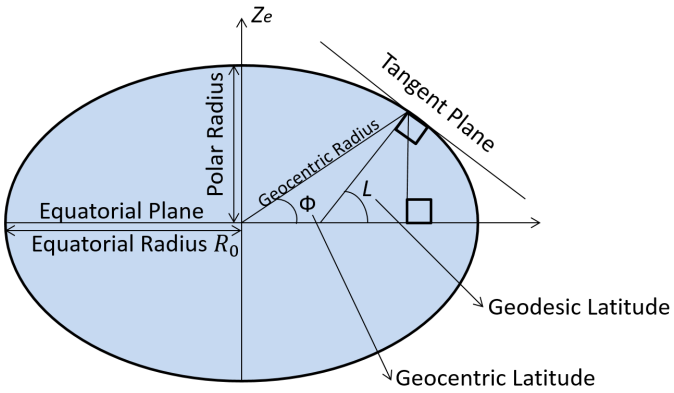

Figure 3 – WGS84 ellipsoid and latitudes definitions.

The geodesic latitude is the one used by GPS and Google Earth tool (Google, 2016), so this paper also uses it to define the geodesic coordinate system e. Being normal to the tangent plane, L and λ may be calculated from the gradient of the traveled distance.

$$dN = R.dL \text{ and } dE = R.cos(L).d\lambda \tag{2}$$

The dN and dE are the traveled distances along the X and Y axis of n, dL and $d\lambda$ are the variation of latitude and longitude, respectively. Due to the ellipsoid shape of the Earth, the radius R used on expression 2 are not the same in each equation. For $d\lambda$, the "meridian radius of curvature" R_N is used, while for dL, the "transverse radius of curvature" R_E is applied. They are given by (Farrell, 2008):

$$R_N(L) = \frac{R_0.(1-e^2)}{(1-e^2.sen^2(L))^{\frac{3}{2}}} \text{ and } R_E(L) = \frac{R_0}{(1-e^2.sen^2(L))^{\frac{1}{2}}} \tag{3}$$

The $\frac{dR_M}{dL}$ and $\frac{dR_E}{dL}$ derivatives during the maneuvers are negligible, so R_N and R_E are calculated once, when the maneuver starts, using the initial latitude L_0. The vehicle's depth d is directly measured by its depth gauge. Finally, the expression that converts vehicle's velocity $\boldsymbol{v_b}$ measured by the DVL sensor and uses the attitude state vector $\boldsymbol{\Theta}$, estimated by the AHRS sensor, to estimate the geodesic position (L, λ, d) of the vehicle is:

$$\boldsymbol{p_e}(t) = \begin{pmatrix} L \\ \lambda \\ d \end{pmatrix}(t) = \begin{pmatrix} \int_0^t \frac{v_{north}(\tau)}{R_M(L_0)} d\tau \\ \int_0^t \frac{v_{east}(\tau)}{cos(L_0).R_N(L_0)} d\tau \\ d(t) \end{pmatrix} + \begin{pmatrix} L_0 \\ \lambda_0 \\ 0 \end{pmatrix} \tag{4}$$

1.2 Correction of magnetic declination

The X axis of n frame points towards the geographic north, a requirement for the conversion of $\boldsymbol{p_n}$ to $\boldsymbol{p_e}$, as showed in expression 4. However, the AHRS sensor, responsible for the heading estimation, uses magnetometers, gyroscopes and accelerometers to perform it. For that reason, it uses the magnetic north as reference, which is different from the geographic north by an angle called "magnetic declination", that varies along the globe.

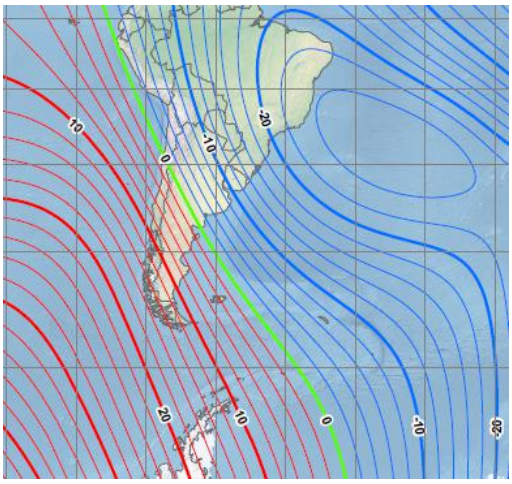

Figure 4 – Magnetic declination in Brazil region (NOAA, 2015).

Figure 4 indicates that, on São Paulo region, the magnetic declination is about -20 deg, which means that it is necessary to subtract 20 deg from the magnetic north heading, estimated by the AHRS, to obtain the geographic north. A more precise value for the magnetic declination on a region can be achieved from many GPS receivers, that determines it according the geodesic position of the vehicle.

1.3 Improvement of velocity measurement and prediction

As the expressions 1 and 4 reveal, the precision of position estimation by the navigation algorithm based on the dead-reckoning principle relies mainly on the precision of the velocity $\boldsymbol{v_b}$ measured by the DVL sensor, and of attitude estimation $\boldsymbol{\Theta}$ by the AHRS sensor. Knowing that, spikes on the velocity measurements were detected, which cause fakes displacements on the trajectory estimation, as presented on fgures 5 and 6.

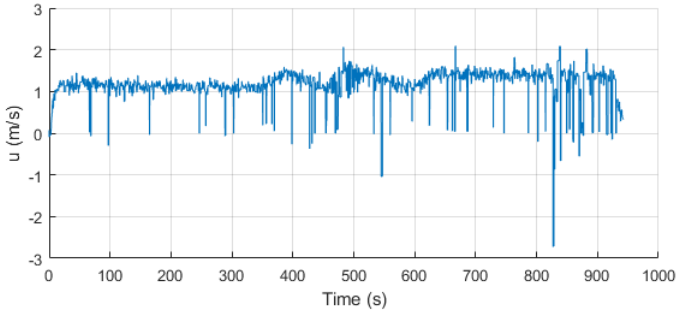

Figure 5 – Spikes on u component of velocity measurement v_b by the DVL sensor.

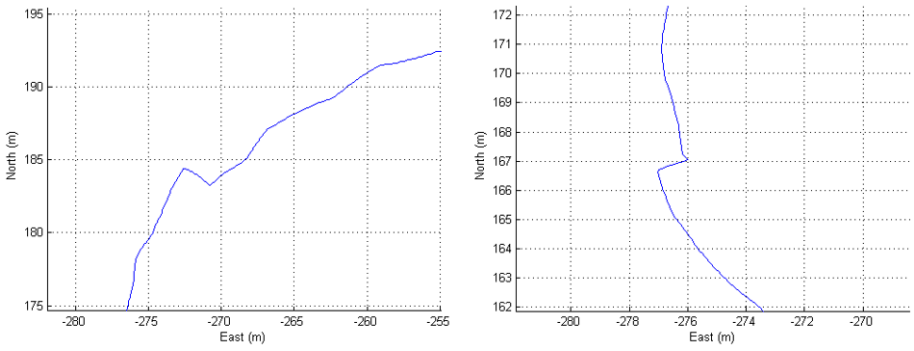

Figure 6 – Fake trajectory displacement due to time integration of spikes on the velocity measurement v_b .

To minimize the presence of spikes on the velocity measurements, it was developed a filter that estimates the speed of the vehicle by integrating in time the linear acceleration measured by the IMU. To bypass the problem of divergence related to noise integration on the acceleration measurements, time integration boundaries are placed between the last velocity estimation and the moment that the filter is supposed to predict. If the difference between the filter's prediction and the current DVL measurement is bigger than a specific value, the measurement is considered as noisy and replaced by the estimation. To avoid instability, the filter has a limited number of times to reject the velocity measurements consecutively. If it reaches this limit, the filter is considered as unstable and diverging from the real value, so the DVL output is reconsidered as valid. The velocity estimation $\hat{\boldsymbol{v}}_{\boldsymbol{b}}$ equation is presented below.

The accelerometer output is normalized by its proof mass magnitude, so it measures the specific force $\boldsymbol{f}$, defined as the non-gravitational force per unit mass, measured in $meters/second^2$ ($m.s^{-2}$):

$\boldsymbol{f} = \boldsymbol{a_i} - \boldsymbol{g}$, where $\boldsymbol{a_i}$ is the acceleration in an inertial frame i and $\boldsymbol{g}$ is the gravitation.

Frame n is non inertial, as Earth is turning with $\Omega \approx \frac{2\pi}{24}\frac{rad}{hour}$. Because of that, fictional forces appear and must be eliminated before acceleration integration. The vehicle's acceleration expressed on frame n is given by (Titterton and Weston, 2004):

$$\boldsymbol{a_n} = \boldsymbol{f} - 2.\boldsymbol{\Omega} \times \boldsymbol{v_n} + \boldsymbol{g_l} \tag{5}$$

where $\boldsymbol{g_l}$ is the local gravity vector, gave by:

$\boldsymbol{g_l} = \boldsymbol{g} - \boldsymbol{\Omega} \times \left(\boldsymbol{\Omega} \times \boldsymbol{r}\right)$, where $\boldsymbol{r}$ is the distance between the center of the Earth and the vehicle.

The velocity estimation $\hat{\boldsymbol{v_n}}$ may be calculated by integrating in time the expression 5. However, the DVL sensor express the velocity on the b frame, so $\hat{\boldsymbol{v_n}}$ must be rotated to b using the matrix $\mathbf{R}_{\mathbf{b}}^{\mathbf{n}}$, which is the inverse of $\mathbf{R}_{\mathbf{b}}^{\mathbf{n}}$, as presented on expression 1. Using a discrete notation for time (k and j integers with $k > j$), $\hat{\boldsymbol{v_b}}$ can be calculated by:

$$\begin{aligned}&\hat{\boldsymbol{v}}_{\boldsymbol{b}}(t_k) = (\mathbf{R}_{\mathbf{b}}^{\mathbf{n}}(\boldsymbol{\Theta}(t_k)))^{-1}.\hat{\boldsymbol{v}}_{\boldsymbol{n}}(t_k) = \\ &(\mathbf{R}_{\mathbf{b}}^{\mathbf{n}}(\boldsymbol{\Theta}(t_k)))^{-1}.\int_{t_{k-j}}^{t_k}[\boldsymbol{f}(\tau) - 2.\boldsymbol{\Omega} \times \boldsymbol{v_n}(\tau) + \boldsymbol{g} - \boldsymbol{\Omega} \times \left(\boldsymbol{\Omega} \times \boldsymbol{r}(\tau)\right)]d\tau + \boldsymbol{v_b}(t_{k-j})\end{aligned} \tag{6}$$

The term $-2.\boldsymbol{\Omega} \times \boldsymbol{v_n}$ is too small and can be rejected. For $u \approx 1,5\ m/s$, its value is:

$$-2.\boldsymbol{\Omega} \times \boldsymbol{v_n} \approx -2.\begin{bmatrix}0 & 0 & \frac{2\pi}{24}\frac{rad}{s^2}\end{bmatrix}^T \times \begin{bmatrix}1,5 & 0 & 0\end{bmatrix}^T \approx \begin{bmatrix}0 & -2,2.10^{-4}m/s^2 & 0\end{bmatrix}^T$$

Finally, the expression 6 is simplified and yields the final equation used by the filter to perform the velocity estimation $\hat{\boldsymbol{v}}_{\boldsymbol{b}}$:

$$\hat{\boldsymbol{v_b}}(t_k) = (\mathbf{R}_{\mathbf{b}}^{\mathbf{n}}(\boldsymbol{\Theta}(t_k)))^{-1}.\int_{t_{k-j}}^{t_k}(\boldsymbol{f}(\tau) + \boldsymbol{g} - \boldsymbol{\Omega} \times \left[\boldsymbol{\Omega} \times \boldsymbol{r}(\tau)\right])d\tau + \boldsymbol{v_b}(t_{k-j}) \tag{7}$$

To compare the expression 7 with the DVL measurements, it is important to remember that its measurement center is different than the one of the IMU. Consequently, it is necessary to translate the DVL velocity to the center of the IMU. According to the Coriolis theorem:

$\boldsymbol{v}_{IMU} = \boldsymbol{v}_{DVL} + \boldsymbol{\Omega}_{IMU} \times \boldsymbol{r}_{DVL,IMU}$, where $\boldsymbol{r}_{DVL,IMU}$ is the distance between the DVL and IMU centers.

This operation, however, in neglected due to minimal precision gain.

2 EVALUATION OF POSITION ERROR ACCUMULATION BY THE NAVIGATION SYSTEM USING ANALYTIC EXPRESSIONS

Evaluating the performance of the navigation algorithm, expressions 1 and 4, can be done by comparing them to GPS position estimation. For that, the vehicle usually must be emerged. However, conducting the vehicle on the surface of the sea imposes different dynamics to the vehicle, related to the case when it operates underwater. Instead of that, it is used only the final GPS position estimation of the AUV, after it has emerged. It is then defined the relative position error, which is the difference between the final navigation algorithm prediction and the final GPS estimation dived by the distance traveled.

This method can evaluate how precise the position estimation is, but can not evaluate its efficiency. The more precise the sensors used, the more precise the position estimation should be. To check if the algorithm is efficiently converting sensor's information in position, it was developed an analytical expression to foresee the relative position error based on sensor's manufactures specifications.

2.1 Error model

Position estimation on n frame $\hat{\boldsymbol{p}}_{\boldsymbol{n}}(t)$ can be represented by its real value $\boldsymbol{p}_{\boldsymbol{n}}(t)$ plus its estimation error $\delta\boldsymbol{p}_{\boldsymbol{n}}(t)$. As presented by expression 1, it is the result of time integration of velocity estimation $\hat{\boldsymbol{v}}_{\boldsymbol{n}}$ on frame n:

$$\hat{\boldsymbol{p}}_{\boldsymbol{n}}(t) = \int_0^t \hat{\boldsymbol{v}}_{\boldsymbol{n}}(\tau)d\tau \text{ where } \hat{\boldsymbol{p}}_{\boldsymbol{n}}(t) = \boldsymbol{p}_{\boldsymbol{n}}(t) + \delta\boldsymbol{p}_{\boldsymbol{n}}(t) \text{ and } \hat{\boldsymbol{v}}_{\boldsymbol{n}}(t) = \boldsymbol{v}_{\boldsymbol{n}}(t) + \delta\boldsymbol{v}_{\boldsymbol{n}}(t)$$

It is deduced then that $\delta\boldsymbol{p}_{\boldsymbol{n}}$ is the result of the velocity error $\delta\boldsymbol{v}_{\boldsymbol{n}}$ integration:

$$\boldsymbol{p}_{\boldsymbol{n}}(t) = \int_0^t \boldsymbol{v}_{\boldsymbol{n}}(\tau)d\tau \text{ and } \delta\boldsymbol{p}_{\boldsymbol{n}}(t) = \int_0^t \delta\boldsymbol{v}_{\boldsymbol{n}}(\tau)d\tau \tag{8}$$

So, to evaluate position error $\delta\boldsymbol{p}_{\boldsymbol{n}}$, it is necessary to develop $\delta\boldsymbol{v}_{\boldsymbol{n}}$ expression. Reapplying expression 1 to 8:

$$\hat{\boldsymbol{v}}_{\boldsymbol{n}}(t) = \hat{\mathbf{R}}^{\mathbf{n}}_{\mathbf{b}}(t).\hat{\boldsymbol{v}}_{\boldsymbol{b}}(t),\ \boldsymbol{v}_{\boldsymbol{n}}(t) + \delta\boldsymbol{v}_{\boldsymbol{n}}(t) = \hat{\mathbf{R}}^{\mathbf{n}}_{\mathbf{b}}(t).(\boldsymbol{v}_{\boldsymbol{b}}(t) + \delta\boldsymbol{v}_{\boldsymbol{b}}(t)) \Rightarrow \delta\boldsymbol{v}_{\boldsymbol{n}}(t) = \hat{\mathbf{R}}^{\mathbf{n}}_{\mathbf{b}}(t).(\boldsymbol{v}_{\boldsymbol{b}}(t) + \delta\boldsymbol{v}_{\boldsymbol{b}}(t)) - \mathbf{R}^{\mathbf{n}}_{\mathbf{b}}(t).\boldsymbol{v}_{\boldsymbol{b}}(t)$$

Finally:

$$\delta v_n(t) = (\hat{R}^n_b(t) - R^n_b(t)).v_b(t) + \hat{R}^n_b(t).\delta v_b(t)) \tag{9}$$

Defining $\hat{\phi} = \phi + \delta\phi$, $\hat{\theta} = \theta + \delta\theta$ and $\hat{\psi} = \psi + \delta\psi$, representing the Euler angles estimation, and applying it to $\mathbf{R}^{\mathbf{n}}_{\mathbf{b}}$ definition on expression 1, it is possible to define $\hat{\mathbf{R}}^{\mathbf{n}}_{\mathbf{b}}(\mathbf{t})$:

$$\hat{\mathbf{R}}^{\mathbf{n}}_{\mathbf{b}}(t) = \begin{pmatrix} c\hat{\theta}.c\hat{\psi} & -s\hat{\psi}.c\hat{\phi} + c\hat{\psi}.s\hat{\theta}.s\hat{\phi} & s\hat{\psi}.s\hat{\phi} + c\hat{\psi}.s\hat{\theta}.c\hat{\phi} \\ c\hat{\theta}.s\hat{\psi} & c\hat{\psi}.c\hat{\phi} + s\hat{\psi}.s\hat{\theta}.s\hat{\phi} & -c\hat{\psi}.s\hat{\phi} + s\hat{\psi}.s\hat{\theta}.c\hat{\phi} \\ -s\hat{\theta} & c\hat{\theta}.s\hat{\phi} & c\hat{\phi}.c\hat{\theta} \end{pmatrix} \tag{10}$$

To expand equation 10, the trigonometric identity of sum may be used:

$$\begin{aligned} cos(\alpha \pm \delta\alpha) &= cos(\alpha).cos(\delta\alpha) \mp sen(\alpha).sen(\delta\alpha) \\ sen(\alpha \pm \delta\alpha) &= sen(\alpha).cos(\delta\alpha) \pm cos(\alpha).sen(\delta\alpha) \end{aligned} \tag{11}$$

It is possible to calculate $\hat{\mathbf{R}}^{\mathbf{n}}_{\mathbf{b}}(\mathbf{t})$ by applying equation 11 on 10. Still, the resulting equation is too large to be analytically presented. Therefore, some simplifications are proposed.

2.2 Simplifying approximations

Simplifying approximations will be presented in order to achieve an analytical expressions for $\delta\boldsymbol{v}_{\boldsymbol{n}}$, as defined on equation 9. The final expression will be based on the navigation sensors error specifications $\delta\boldsymbol{v}_{\boldsymbol{b}} = \begin{pmatrix}\delta v_x & \delta v_y & \delta v_z\end{pmatrix}^T$ and $\delta\boldsymbol{\Theta} = \begin{pmatrix}\delta\phi & \delta\theta & \delta\psi\end{pmatrix}^T$, DVL and AHRS accuracy, respectively.

1. **Small-angles approximation:**
   Taking $\delta\alpha$, defined on expression 11, as small enough (usually adopted as less than $5deg$), it is possible to simplify the basic trigonometric functions without significant loss of precision. The approximation considers $sin(\delta\alpha) \approx \delta\alpha$ and $cos(\delta\alpha) \approx 1$. So, expression 11 becomes:

   $$\begin{aligned} cos(\alpha \pm \delta\alpha) &\approx cos(\alpha) \mp sen(\alpha).\delta\alpha \\ sen(\alpha \pm \delta\alpha) &\approx sen(\alpha) \pm cos(\alpha).\delta\alpha \end{aligned} \tag{12}$$

   Specifically for the Pirajuba AUV case, its AHRS manufacturer guarantees an accuracy RMS of ± 0.45 *deg* for *roll* and *pitch*, and of ± 1.0 *deg* for *yaw*. So, the terms of 10 become:

   $$\begin{aligned} &c\hat{\theta} \approx c\theta - s\theta.\delta\theta,\ s\hat{\theta} \approx s\theta + c\theta.\delta\theta \\ &c\hat{\phi} \approx c\phi - s\phi.\delta\phi,\ s\hat{\phi} \approx s\phi + c\phi.\delta\phi \\ &c\hat{\psi} \approx c\psi - s\psi.\delta\psi,\ s\hat{\psi} \approx s\psi + c\psi.\delta\psi \end{aligned} \tag{13}$$

   Applying expressions 13 on 10, it is possible to reduce the analytical expression for δv_n, but it is still too large to be presented here. So, a second approximation is proposed.

2. **First-order approximation:** The velocity error δv_n of expression 9 depends on the error terms $\delta\boldsymbol{v}_{\boldsymbol{b}} = \begin{pmatrix}\delta v_x & \delta v_y & \delta v_z\end{pmatrix}^T$ and $\delta\boldsymbol{\Theta} = \begin{pmatrix}\delta\phi & \delta\theta & \delta\psi\end{pmatrix}^T$, which are the accuracy of the navigation sensors of velocity, DVL, and of attitude, AHRS. Following the small-angles approximation, it is possible to reject all the second-order, or higher, terms of error, leaving only first-order error terms. The $\hat{\mathbf{R}}^{\mathbf{n}}_{\mathbf{b}}$, expression 10, becomes:

Element (i,j)	Original	Approximation
$(1,1)$	$c\hat{\theta}.c\hat{\psi}$	$c\theta.c\psi - c\psi.\delta\theta.s\theta - c\theta.\delta\psi.s\psi$
$(1,2)$	$-s\hat{\psi}.c\hat{\phi} + c\hat{\psi}.s\hat{\theta}.s\hat{\phi}$	$-c\phi.c\psi.\delta\psi + c\phi.c\psi.\delta\phi.s\theta + c\theta.c\psi\delta\theta.s\phi + c\psi.s\theta s\phi$ $-c\phi.s\psi + \delta\phi.s\phi.s\psi - \delta\psi.s\theta.s\phi.s\psi$
$(1,3)$	$s\hat{\psi}.s\hat{\phi} + c\hat{\psi}.s\hat{\theta}.c\hat{\phi}$	$c\theta.c\phi.c\psi.\delta\theta + c\phi.c\psi.s\theta + c\psi.\delta\psi.s\phi$ $-c\psi.\delta\phi.s\theta.s\phi + c\phi.\delta\phi.s\psi - c\phi\delta\psi.s\theta.s\psi + s\phi.s\psi$
$(2,1)$	$c\hat{\theta}.s\hat{\psi}$	$c\theta.c\psi.\delta\psi + c\theta.s\psi - \delta\theta.s\theta.s\psi$
$(2,2)$	$c\hat{\psi}.c\hat{\phi} + s\hat{\psi}.s\hat{\theta}.s\hat{\phi}$	$c\phi.c\psi - c\psi.\delta\phi.s\phi + c\psi.\delta\psi.s\theta.s\phi$ $-c\phi.\delta\psi.s\psi + c\phi.\delta\phi.s\theta.s\psi + c\theta.\delta\theta.s\phi s\psi + s\theta.s\phi.s\psi$
$(2,3)$	$-c\hat{\psi}.s\hat{\phi} + s\hat{\psi}.s\hat{\theta}.c\hat{\phi}$	$-c\phi.c\psi.\delta\phi + c\phi.c\psi.\delta\psi.s\theta - c\psi.s\phi + c\theta.c\phi.\delta\theta.s\psi$ $+c\phi.s\theta.s\psi + \delta\psi.s\phi.s\psi - \delta\phi.s\theta.s\phi.s\psi$
$(3,1)$	$-s\hat{\theta}$	$-c\theta.\delta\theta - s\theta$
$(3,2)$	$c\hat{\theta}.s\hat{\phi}$	$c\theta.c\phi.\delta\phi + c\theta.s\phi - \delta\theta.s\theta.s\phi$
$(3,3)$	$c\hat{\phi}.c\hat{\theta}$	$c\theta.c\phi - c\phi.\delta\theta.s\theta - c\theta.\delta\phi.s\phi$

Table 1 – Simplification of matrix $\hat{\mathbf{R}}_{\mathbf{b}}^{\mathbf{n}}(t)$ using first-order errors approximation.

Expanding expression 9 using $\hat{\mathbf{R}}_{\mathbf{b}}^{\mathbf{n}}$, defined on table 1, and re-applying first-order approximation results on it, the analytical simplified expression for $\delta\boldsymbol{v_n} = \begin{pmatrix}\delta v_{north} & \delta v_{east} & \delta v_{down}\end{pmatrix}^T$ become:

$$\begin{aligned}
\delta v_{north} &= c\theta.c\psi.\delta v_x + (c\psi.s\theta.s\phi - c\phi.s\psi).\delta v_y + (c\phi.c\psi.s\theta + s\phi.s\psi)\delta v_z + \dots \\
&\dots[(c\phi.c\psi.s\theta + s\phi.s\psi)v_y + (c\phi.s\psi - c\psi.s\theta.s\phi)v_z]\delta\phi + (-c\psi.s\theta.v_x + c\theta.c\psi.s\phi.v_y + c\theta.c\phi.c\psi.v_z)\delta\theta + \dots \\
&\dots[-c\theta.s\psi.v_x + (-c\phi.c\psi - s\theta.s\phi.s\psi)v_y + (c\psi.s\phi - c\phi.s\theta.s\psi)v_z]\delta\psi, \\
\delta v_{east} &= c\theta.s\psi.\delta v_x + (s\theta.s\phi.s\psi + c\phi.c\psi)\delta v_y + (c\phi.s\theta.s\psi - c\psi.s\phi)\delta v_z + \dots \\
&\dots[(c\phi.s\theta.s\psi - c\psi.s\phi)v_y + (-c\phi.c\psi - s\theta.s\phi.s\psi)v_z)]\delta\phi + (-s\theta.s\psi.v_x + c\theta.s\phi.s\psi.v_y + c\theta.c\phi.s\psi.v_z)\delta\theta + \dots \\
&\dots[c\theta.c\psi.v_x + (c\psi.s\theta.s\phi - c\phi.s\psi)v_y + (s\phi.s\psi + c\phi.c\psi.s\theta)v_z]\delta\psi, \\
\delta v_{down} &= -s\theta.\delta v_x + c\theta.s\phi.\delta v_y + c\theta.c\phi.\delta v_z + (c\theta.c\phi.v_y - c\theta.s\phi.v_z)\delta\phi + (-c\theta.v_x - s\theta.s\phi.v_y - c\phi.s\theta.v_z)\delta\theta
\end{aligned} \tag{14}$$

Expression 14 is still considerably large, but can be used to predict the accuracy of position estimation by dead reckoning algorithm, as presented on equations 4 and 8, using the manufacturers specifications of the navigations sensors. Furthers simplifications can be considered depending on the manner the AUV navigates.

3. **Negligible roll and horizontal plane:** If the AUV navigates with negligible roll or limited to an horizontal plane, furthers simplifications can be adopted. In those cases, it is possible to consider the vehicle's roll $\phi \approx 0$ and pitch $\theta \approx 0$.

   For negligible roll $\phi \approx 0$, that is, $c\phi \approx 1$ and $s\phi \approx 0$, expression 14 becomes:

$$\begin{aligned}
\delta v_{north} &= c\theta.c\psi.\delta v_x - s\psi.\delta v_y + c\psi.s\theta.\delta v_z + \dots \\
&\dots(c\psi.s\theta.v_y + s\psi.v_z)\delta\phi + (-c\psi.s\theta.v_x + c\theta.c\psi.v_z)\delta\theta + (-c\theta.s\psi.v_x - c\psi.v_y - s\theta.s\psi.v_z)\delta\psi, \\
\delta v_{east} &= c\theta.s\psi.\delta v_x + c\psi.\delta v_y + s\theta.s\psi.\delta v_z + \dots \\
&\dots(s\theta.s\psi.v_y - c\psi.v_z)\delta\phi + (-s\theta.s\psi.v_x + c\theta.s\psi.v_z)\delta\theta + (c\theta.c\psi.v_x - s\psi.v_y + c\psi.s\theta.v_z)\delta\psi, \\
\delta v_{down} &= -s\theta.\delta v_x + c\theta.\delta v_z + c\theta.v_y.\delta\phi + (-c\theta.v_x - s\theta.v_z)\delta\theta
\end{aligned} \tag{15}$$

   Considering an horizontal plane for the maneuver, it is possible to impose pitch $\theta \approx 0$, that is, $c\theta \approx 1$ and $s\theta \approx 0$. Than, expression 14 becomes:

$$\begin{aligned}
\delta v_{north} &= c\psi.\delta v_x - c\phi.s\psi.\delta v_y + s\phi.s\psi.\delta v_z + \dots \\
&\dots(s\phi.s\psi.v_y + c\phi.s\psi.v_z)\delta\phi + (c\psi.s\phi.v_y + c\phi.c\psi.v_z)\delta\theta + (-s\psi.v_x - c\phi.c\psi.v_y + c\psi.s\phi.v_z)\delta\psi, \\
\delta v_{east} &= s\psi.\delta v_x + c\phi.c\psi.\delta v_y - c\psi.s\phi.\delta v_z + \dots \\
&\dots(-c\psi.s\phi.v_y - c\phi.c\psi.v_z)\delta\phi + (s\phi.s\psi.v_y + c\phi.s\psi.v_z)\delta\theta + (c\psi.v_x - c\phi.s\psi.v_y + s\phi.s\psi.v_z).\delta\psi, \\
\delta v_{down} &= s\phi.\delta v_y + c\phi.\delta v_z + (c\phi.v_y - s\phi.v_z)\delta\phi - v_x.\delta\theta
\end{aligned} \tag{16}$$

   Considering both simplification simultaneously, that is, roll $\phi \approx 0$ and pitch $\theta \approx 0$, the expression 14 becomes:

$$\begin{aligned}
\delta v_{north} &= c\psi.\delta v_x - s\psi.\delta v_y + s\psi.v_z.\delta\phi + c\psi.v_z.\delta\theta + (-s\psi.v_x - c\psi.v_y)\delta\psi, \\
\delta v_{east} &= s\psi.\delta v_x + c\psi.\delta v_y - c\psi.v_z.\delta\phi + s\psi.v_z.\delta\theta + (c\psi.v_x - s\psi.v_y)\delta\psi, \\
\delta v_{down} &= \delta v_z + v_y.\delta\phi - v_x.\delta\theta
\end{aligned} \tag{17}$$

Results

The filter for velocity measurement, expression 7, performed correctly, eliminating important spikes and fake trajectory displacements.

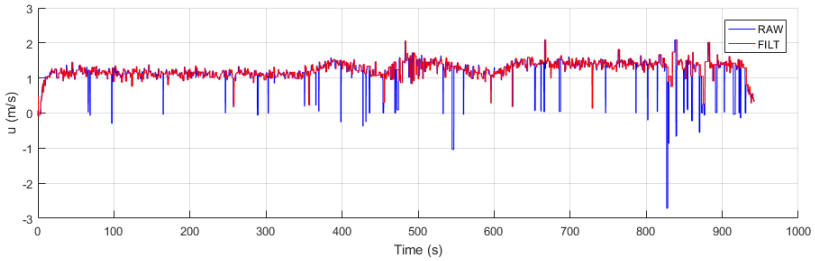

Figure 7 – Filter results for u component of velocity v_b.

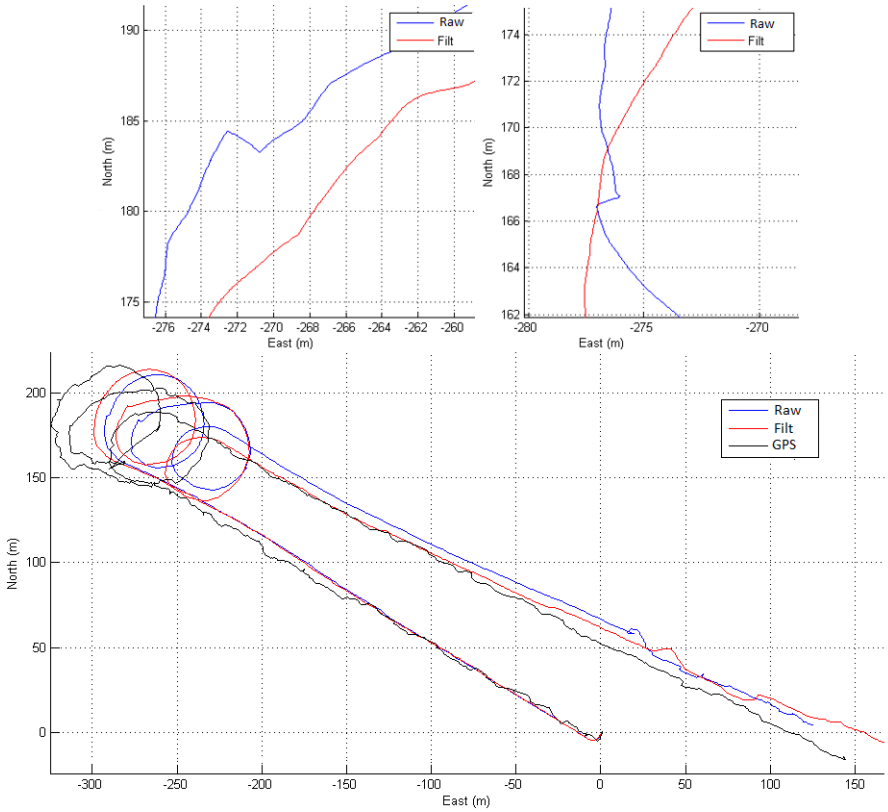

Figure 8 – Filter results for vehicle's position.

The algorithm for position estimation presented by expressions 1 and 4 were tested using real navigation data collected by the Pirajuba AUV on the northern coastline of São Paulo, Brazil. The maneuvers were conducted both underwater and on the surface of the sea, for GPS signal acquisition. For the first case, there is no GPS signal available throughout the trajectory, but its start and final positions, since the vehicle is emerged, do have access to GPS position estimation, which can be used as reference for the performance study of the algorithm. There is, though, a delay, required for synchronization between the receiver and the satellite constellation, which can vary from a few seconds to a few minutes. That fact degenerates progressively the reliability of the GPS as reference, as the vehicle is naturally drifting during it. For the second case, when the vehicle is navigating on the surface of the water, the GPS signal is available throughout the mission, enabling comparison on any point of the trajectory. However, the AUV dynamics in this case are different than on its real application undersea. As show on figure 9, one of the rudders stays useless out of water. Also, the elevators have to impose a pitch $\theta > 0$ to prevent the GPS antenna to get covered by the water. Wind and waves can likewise disturb the vehicle and so on. Both cases are presented.

Figure 9 – Pirajuba AUV during a maneuver on the surface of the sea, for GPS signal acquisition.

Expression 1 plots the maneuver in a local navigation frame.

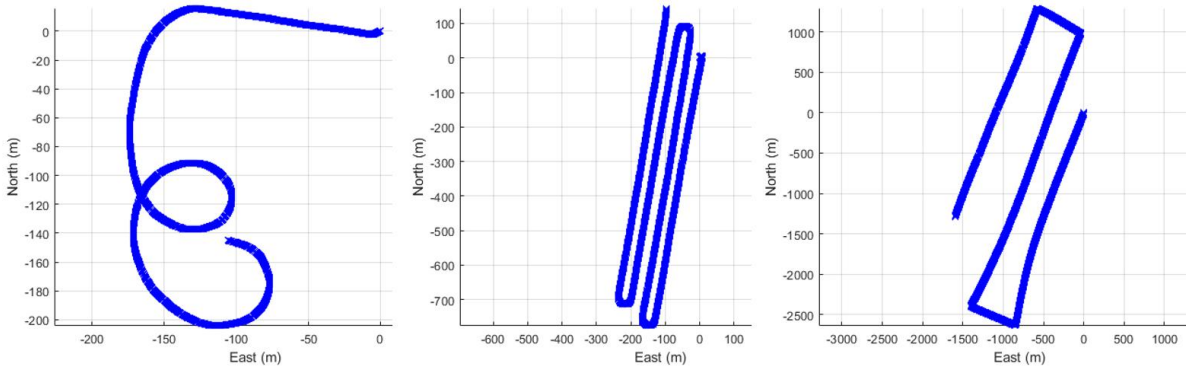

Figure 10 – Maneuvers 1 (left), 2 (center) and 3 (right) plotted on frame n. Start points at $(0,0)$.

Maneuvers duration t and distances traveled d are: $t_1 \approx 11$ *min*, $d_1 \approx 650$ *m*, $t_2 \approx 49$ *min*, $d_2 \approx 3\,543$ *m* and $t_3 \approx 2h$ 22 *min*, $d_3 \approx 10\,752$ *m*. Using expression 4, it is possible to convert the estimated trajectory to geodesic coordinates and plot it on Google Earth maps (Google, 2016), using the library "Google Earth Toolbox" for Matlab developed by Davis (2012). Maneuver was conducted on the surface of the sea and have GPS position estimation throughout the trajectory.

Figure 11 – Maneuvers 1 (left), 2 (center) and 3 (right) plotted on frame e using Google Earth tool (Google, 2016).

To evaluate the performance of the navigation algorithm, the GPS position estimation is adopted as reference. The algorithm's error is defined as the difference between the GPS and the algorithm final position estimation. This value is absolute (meters) and must be divided by the total traveled distance to provide the relative error (%), which express the performance of the algorithm.

The results of the analytical expressions for the accumulated positioning error estimation, equations 14 to 17, are

also presented and compared to the navigation algorithm's relative error. For the terms $\delta \boldsymbol{v_b}$ and $\delta \boldsymbol{\Theta}$, the navigation sensors errors, the following values are adopted based on manufacturers specifications and augmented by a fraction to represent others errors sources: $\delta \boldsymbol{v_b} = \begin{pmatrix} \delta v_x & \delta v_y & \delta v_z \end{pmatrix}^T = \begin{pmatrix} 5\%.v_x & 5\%.v_y & 5\%.v_z \end{pmatrix}^T$ and $\delta \boldsymbol{\Theta} = \begin{pmatrix} \delta\phi & \delta\theta & \delta\psi \end{pmatrix}^T = \begin{pmatrix} 3deg & 3deg & 3deg \end{pmatrix}^T$. For the real values of $\boldsymbol{v_b} = \begin{pmatrix} v_x & v_y & v_z \end{pmatrix}^T$ and $\boldsymbol{\Theta} = \begin{pmatrix} \phi & \theta & \psi \end{pmatrix}^T$, there is obviously no direct access . To work around that, it is adopted $\boldsymbol{v_b} \approx \hat{\boldsymbol{v}}_{\boldsymbol{b}}$ and $\boldsymbol{\Theta} \approx \hat{\boldsymbol{\Theta}}$, which means that the real values are approximately equal to the measured ones. This approximation permits to obtain the positioning error estimation, since the main terms of the analytical expressions are actually $\delta \boldsymbol{v_b}$ and $\delta \boldsymbol{\Theta}$. The following table 2 presents the results for maneuvers 1 to 3.

Maneuver Number	Algorithm's relative error	Relative error prediction eq. 14	Relative error prediction eq. 15	Relative error prediction eq. 16	Relative error prediction eq. 17
1	3.2%	2.6%	2.6%	2.6%	2.6%
2	1.6%	0.5%	0.5%	0.5%	0.5%
3	2.8%	2.3%	2.4%	2.4%	2.4%

Table 2 – Comparison of maneuver's relative errors, real and by prediction.

CONCLUSIONS

Due to lack of GPS signal underwater, AUVs require a reliable navigation system, in order to navigate autonomously. The navigation system is responsible for attitude and linear position estimation and its precision defines the vehicle's autonomy. The better the quality of the navigation sensors, the better the accuracy of the algorithm; but there are also others important points to observe, like reliable dynamic and kinematic equations and treatment of disturbing physical effects. This paper used the dead reckoning principle to estimate the vehicle's position, expressing it on local and geodesic frames. Magnetic declination and improvement of velocity measurement were identified as key points to improve algorithm performance.

The navigation algorithm has successfully estimated vehicle's position, with a relative error under 3.5%. Similarly, the velocity filter eliminated spikes from DVL measurements, avoiding fake displacements on the trajectory. The conversion of position estimation for geodesic coordinates during underwater maneuvers is useful for oceanographic data correlation with maps and for missions improvements analysis, using Google Earth (Google, 2016) as an important tool for visualization. Positioning error prediction by analytic expression is important for navigation algorithm performance analysis and for embedded predication, so the vehicle can foresee the moment to emerge for position correction using GPS signal. The analytics expressions presented here vary according approximations hypothesis assumptions. For maneuvers on horizontal plane, like those presented, no considerable loss of precision was identified between each of the error predictions. In this case, it is suggested to use the lean one, expression 17, since it takes less computational resources to be executed, an important aspect if it has to be embedded on the vehicle with real time restrictions.

Since real world has lot of variables, tuning the navigation system is a continuous work. The author emphasizes this point here, so the navigations systems could achieve progressively better results, not relying strictly on the improvement of navigation sensors accuracy. As a suggestion, some other points to be considered are: sensor calibration, sensor alignment, signal processing and increase of discretization rate.

REFERENCES

Barros, E. et al., 2008, "Investigation of normal force and moment coefficients for an auv at nonlinear angles of attack and sideslip range", IEEE Journal of Oceanic Engineering.

Caetano, W., 2014, "Identificação de coeficientes de manobra de veículos submarinos através de testes com modelos livres", Master's thesis, Escola Politécnica da USP.

Davis, S. L., 2012, "Google Earth Toolbox".

Farrell, J. A., 2008, "Aided Navigation - GPS with High Rate Sensors", The McGraw-Hill Companies.

Freire,L.O., 2013, "Desenvolvimento de uma arquitetura de controle descentralizada para veículos submarinos baseada em CAN, ARM e engenharia de sistemas", Master's thesis, Escola Politécnica da USP.

Google, 2016, "Google earth", free software.

NOAA, 2015, "NOAA (National Oceanic and Atmospheric administration) - National Centers for Environmental Information", available in: <http://www.ngdc.noaa.gov/geomag/declination.shtml>

Paull, L. et al., 2014, "AUV navigation and localization: A review", IEEE JOURNAL OF OCEANIC ENGINEERING, 39.

Titterton, D. and Weston, J. L., 2004. "Strapdown Inertial Navigation Technology", IET.

Vivanco, P. J. C., 2014, "Desenvolvimento do sistema de navegação de um auv baseado em filtro estendido de kalman", Master's thesis, Escola Politécnica da USP.

Zanoni, F. D., 2012, "Modelagem e implementação do sistema de navegação para um auv", Master's thesis, Escola Politécnica da USP.